J Intell Robot Syst
DOI 10.1007/s10846-013-9916-5

Real-Time Implementation of Decoupled Controllers for Multirotor Aircrafts

Hao Liu · Danjun Li · Jonghyuk Kim · Yisheng Zhong

Received: 8 August 2013 / Accepted: 12 September 2013

Abstract In this paper, a practical controller design method is presented to control six degrees of freedom multirotor aircrafts–quadrotors. The quadrotor system is divided into four subsystems; that is, the longitudinal, lateral, yaw, and height subsystems. Then, a linear and decoupled nominal model is obtained for each subsystem, whereas coupling and nonlinear dynamics, parametric perturbations, and external disturbances are considered as uncertainties. For each subsystem, a decoupled robust controller is then proposed. Although there exist coupling between each channel, the output tracking errors of the four subsystems are proven to ultimately converge into *a-priori* set neighborhood of the origin. Finally, real-time implementation results of the decoupled controller are given to demonstrate its viability and applicability.

Keywords Multirotor aircrafts · Quadrotors · Decoupled control · Robust control

1 Introduction

In the last decade, there has been an increasing interest in autonomous helicopters for various applications such as surveillance, mapping, exploration, and research [1–4]. The helicopters have several advantages over the fixed wing aircrafts, because of their unique capabilities of hovering, taking-off and landing vertically [5].

Compared to conventional helicopters, multirotor aircrafts are more maneuverable and have more simple mechanism, thus attracting more interests. The quadrotor, which possesses four rotors and is shown in Fig. 1, is regarded as one kind of typical multirotor aircrafts and extensive studies have been made to achieve their automatic flight. The quadrotor is a nonlinear dynamic system with six degrees of freedom (6 DOF). Full dynamic system incorporating 6 DOF was considered in [6], and a Lyapunov-based control algorithm was derived based on the backstepping

H. Liu (✉)
School of Astronautics, Beihang University, Beijing 100191, Peoples Republic of China
e-mail: liuhao13@buaa.edu.cn

H. Liu · D. Li · Y. Zhong
Department of Automation, TNList, Tsinghua University, Beijing 100084, Peoples Republic of China

D. Li
PLA, 61902 Unit, Yibin, Sichuan 644000, Peoples Republic of China

J. Kim
Research School of Engineering, Australian National University, ACT 0200, Australia

Fig. 1 The quadrotor in hover

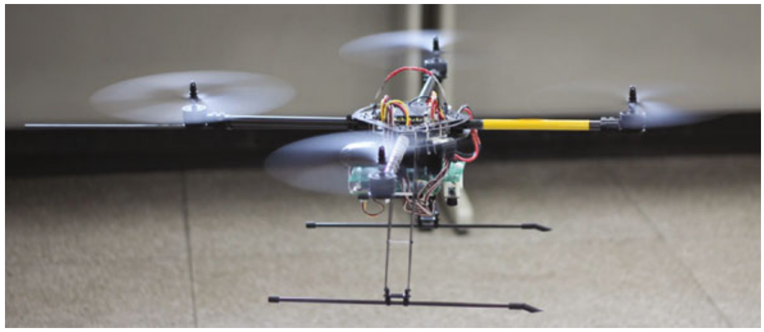

techniques for a small model autonomous helicopter to stabilize over a marked landing pad. In [7], a dynamic model of the quadrotor was obtained by applying the Lagrange modeling method, and a nested saturation control was used for the quadrotor to perform autonomous missions of taking-off and landing vertically. A two-camera method was introduced to estimate the pose information in [8], and a controller using the feedback linearization and backstepping-based approach was proposed for the quadrotor. In [9] and [10], the classic proportional-integral-derivative (PID) controller was investigated to control a quadrotor robot. A partial state feedback control law was designed via the singular perturbation theory for a miniature quadrotor UAV as shown in [11]. However, generally, the quadrotor system is subject to various uncertainties such as parameter perturbations, unmodeled uncertainties, and external disturbances. Therefore, recently, robust control of quadrotors has been focused extensively (see, e.g. [12–15]). However, many of these researches have addressed uncertainties involved in the rotational dynamics of the quadrotors, whereas designing robust controllers against the uncertainties in the full 6-DOF dynamics of these vehicles is still a challenging problem.

In the current paper, the robust position control problem of the quadrotor is investigated. The influence of uncertainties existing in the 6-DOF motion of the vehicle is required to be restrained. Instead of directly dealing with the full nonlinearity, a robust and quite practical decoupled approach is proposed as follows. The quadrotor system is firstly divided into four subsystems, that is, the height subsystem, the longitudinal subsystem, the lateral subsystem, and the yaw subsystem. A linear and decoupled nominal model is then obtained through a system identification for each subsystem, and all uncertainties are included as the equivalent disturbances. Finally, a linear time-invariant and robust controller is proposed for each subsystem.

Compared with the existing works on automatic quadrotor control, the main contributions of the current article are threefold. First, the uncertainties involved in the 6-DOF dynamics can be restrained. For each subsystem, the designed controller consists of a nominal controller to achieve the desired tracking of the nominal model and a robust compensator to restrain the effects of the equivalent disturbances. Second, although three exists coupling between each subsystem, a decoupled control is achieved for the uncertain aerial vehicle. The tracking error of each subsystem is guaranteed to converge into the given neighborhood of the origin ultimately. Lastly, the resulted controller has a form of linear time-invariant and decoupled structure, which is easy to implement and be tuned in practical applications.

The rest of this paper is organized as follows. In Section 2, the four subsystems of the quadrotor is introduced and the linear model of each subsystem is briefly illustrated. The decoupled and robust controller is proposed for each subsystem in Section 3. In Section 4, robustness properties of the whole closed-loop control system are analyzed. Real-time implementation results of the designed controller are given in Section 5. Finally, Section 6 concludes the work with future research directions.

2 Model Description

In this section, the inertial frame and the body fixed frame are introduced. Let $E = \{E_x, E_y, E_z\}$ denote the inertial frame, which is considered fixed to the earth. As depicted in Fig. 2, let $E_b = \{E_{bx}, E_{by}, E_{bz}\}$ be the body fixed frame linked to the quadrotor, which is considered as a rigid body. The origin of the body fixed frame is the mass center of the vehicle. Denote $\xi = [\xi_x\ \xi_y\ \xi_z]^T$ the position of the vehicle expressed in the frame E and $\eta = [\phi\ \theta\ \psi]^T$ the three Euler angles, which determine the quadrotor orientation from E to E_b [15]. ϕ is the roll angle, θ the pitch angle, and ψ the yaw angle as shown in Fig. 2. The quadrotor has four rotors: the front rotor, the back rotor, the left rotor, and the right rotor. By changing the lift forces produced by the four rotors, the quadrotor can achieve various maneuvers. If the rotational speed of the front rotor increases while that of the back rotor decreases, then the vehicle will pitch and thus move longitudinally. The rolling and lateral motions can be achieved similarly by changing the rotational velocities of the left and right rotors. The difference of the counter-torque produced between the front and back rotors and the left and right rotors results in the yawing motion. Finally, the vertical motion can be achieved by changing the total thrust generated by the four rotors. The quadrotor has four control inputs $u_i (i = 1, 2, 3, 4)$ to change the external torques around the axes E_{by}, E_{bx}, and E_{bz} and the total lift force produced by the four rotors respectively.

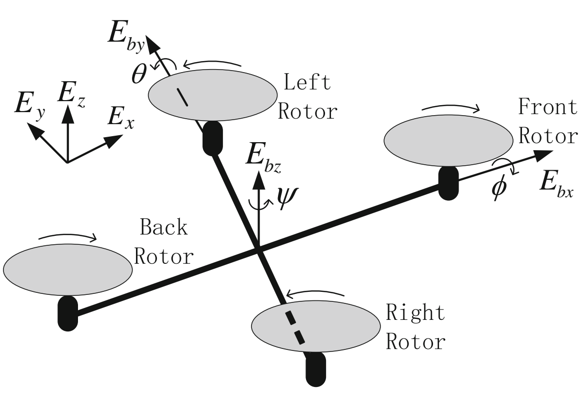

Fig. 2 Schematic of quadrotor

The quadrotor system thus consists of four subsystems: the longitudinal subsystem, the lateral subsystem, the yaw subsystem, and the height (vertical) subsystem. Corresponding inputs and outputs for the four subsystems are u_1 and ξ_x, u_2 and ξ_y, u_3 and ψ, and u_4 and ξ_z, respectively. The nominal model for each subsystem is considered as linear time-invariant (LTI) and its parameters are determined from the system identification process. The dynamics of the longitudinal and lateral subsystems are modeled as the following systems:

$$\begin{aligned}
\ddot{\xi}_x &= a_{0x}\xi_x + a_{1x}\dot{\xi}_x + b_{1x}\theta, \\
\ddot{\theta} &= a_{2x}\theta + a_{3x}\dot{\theta} + b_{2x}u_1, \\
\ddot{\xi}_y &= a_{0y}\xi_y + a_{1y}\dot{\xi}_y + b_{1y}\phi, \\
\ddot{\phi} &= a_{2y}\phi + a_{3y}\dot{\phi} + b_{2y}u_2,
\end{aligned} \tag{1}$$

and the yaw and height subsystems as

$$\begin{aligned}
\ddot{\psi} &= a_{0\psi}\psi + a_{1\psi}\dot{\psi} + b_{\psi}u_3, \\
\ddot{\xi}_z &= a_{0z}\xi_z + a_{1z}\dot{\xi}_z + b_{z}u_4,
\end{aligned} \tag{2}$$

where a_i and b_i are nominal parameters determined from the system identification. From Eqs. 1 and 2, one can see that for each subsystem, only a linear time-invariant and single-input single-output (SISO) model is required, which can be obtained comparatively easily.

Let $r_i (i = x, y, \psi, z)$ be the desired references for ξ_x, ξ_y, ψ, and ξ_z respectively. Then the models can be rewritten in terms of error variables which are defined as $e_x = [e_{x,j}]_{4\times 1}$, $e_y = [e_{y,j}]_{4\times 1}$, $e_\psi = [e_{\psi,j}]_{2\times 1}$, and $e_z = [e_{z,j}]_{2\times 1}$, where $e_{i,1} = \xi_i - r_i (i = x, y, z)$, $e_{\psi,1} = \psi - r_\psi$, $e_{x,3} = \theta + (a_{0x}r_x + a_{1x}\dot{r}_x - \ddot{r}_x)/b_x$, $e_{y,3} = \phi + (a_{0y}r_y + a_{1y}\dot{r}_y - \ddot{r}_y)/b_y$, $e_{i,j} = \dot{e}_{i,j-1} (i = x, y;\ j = 2, 4)$, and $e_{k,2} = \dot{e}_{k,1} (k = \psi, z)$. Let

$$A_i = \begin{bmatrix} 0 & 1 & 0 & 0 \\ a_{0i} & a_{1i} & b_{1i} & 0 \\ 0 & 0 & 0 & 1 \\ 0 & 0 & a_{2i} & a_{3i} \end{bmatrix}, \quad B_i = \begin{bmatrix} 0 \\ 0 \\ 0 \\ b_{2i} \end{bmatrix}, \quad i = x, y,$$

and

$$A_j = \begin{bmatrix} 0 & 1 \\ a_{0j} & a_{1j} \end{bmatrix}, B_j = \begin{bmatrix} 0 \\ b_j \end{bmatrix}, j = \psi, z.$$

Then, the error dynamic model for a single subsystem becomes

$$\dot{e}_i = A_i e_i + B_i(u_i + \Delta_i), i = x, y, \psi, z, \quad (3)$$

where $\Delta_i (i = \theta, \phi, \psi, z)$ are the named equivalent disturbances which involve uncertainties such as coupling and nonlinear dynamics, parametric perturbations, and external disturbances.

By combining all subsystems, one can see that the whole quadrotor error system in a matrix-vector form can be described as

$$\dot{e} = Ae + B(u + \Delta), \quad (4)$$

where $e = \left[e_x^T \ e_y^T \ e_\psi^T \ e_z^T \right]^T$, $u = \left[u_x \ u_y \ u_\psi \ u_z \right]^T$, $\Delta = \left[\Delta_x \ \Delta_y \ \Delta_\psi \ \Delta_z \right]^T$, and

$$A = diag(A_x, A_y, A_\psi, A_z), \ B = diag(B_x, B_y, B_\psi, B_z).$$

Assumption 1 For the equivalent disturbances $\Delta_i (i = 1, 2, 3, 4)$, there exist positive constants ς_{ei}, $\delta_i < 1$, and ς_{ci} such that $\|\Delta_i\|_\infty \le \varsigma_{ei} \|e\|_\infty + \delta_i \|u_i\|_\infty + \varsigma_{ci}$.

This is a reasonable assumption in many practical systems.

3 Decoupled Controller Design

In this paper, the goal of the designed controller is to achieve the desired tracking properties of the closed-loop control system: for *a-priori* set constants ε and a given bounded initial state $e(0)$, there exists a positive constant T, such that the state of the whole quadrotor system is bounded and satisfies that $|e(t)| \le \varepsilon, \forall t \ge T$.

If the uncertainties Δ is ignored, the error model (4) is the nominal model. The control inputs $u_i (i = x, y, \psi, z)$ consists of two parts: the nominal part $u_i^N (i = x, y, \psi, z)$ and the robust compensating part $u_i^R (i = x, y, \psi, z)$ as

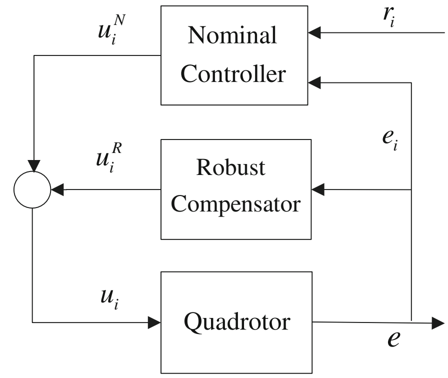

Fig. 3 The schematic diagram of the closed-loop robust control system. It consists of four subsystems: the longitudinal subsystem ($i = x$), the lateral subsystem ($i = y$), the yaw subsystem ($i = \psi$), and the height subsystem ($i = z$)

$$u_i = u_i^N + u_i^R, i = x, y, \psi, z. \quad (5)$$

The nominal inputs are designed for each nominal system to achieve the desired tracking, whereas the robust compensating inputs are introduced to restrain the effects of the uncertainties Δ.

The nominal feedback control laws for the four subsystems are designed based on the static feedback control approach as follows

$$u_i^N = -K_i e_i, i = x, y, \psi, z. \quad (6)$$

Denote $A_{iH} = A_i - B_i K_i (i = x, y, \psi, z)$, where the parameters of the matrix K_i is selected such that A_{iH} is Hurwitz. Then the closed-loop system dynamics becomes

$$\dot{e}_i = A_{iH} e_i + B_i \left(u_i^R + \Delta_i \right), i = x, y, \psi, z. \quad (7)$$

Table 1 Helicopter parameters

Parameter	Value	Parameter	Value	Parameter	Value
a_{0x}	0	a_{1x}	0	b_{1x}	9.81
a_{2x}	0	a_{3x}	0	b_{2x}	9.7
a_{0y}	0	a_{1y}	0	b_{1y}	9.81
a_{2y}	0	a_{3y}	0	b_{2y}	9.2
$a_{0\psi}$	0	$a_{1\psi}$	0	b_ψ	9.81
a_{0z}	0	a_{1z}	0	b_z	9.81

The robust compensating inputs $u_i^R(i = x, y, \psi, z)$ are to be designed to restrain the effects of the equivalent disturbances Δ_i, such that the closed-loop control system could respond as the nominal system $\dot{e}_i = A_{iH}e_i$. However, $\Delta_i(i = x, y, \psi, z)$ cannot be measured directly, and therefore robust filters are introduced (see also in [16]). The robust filters have the following forms

$$F_i(p) = f_i^4/(f_i + p)^4, i = x, y,$$

$$F_j(p) = f_j^2/(f_j + p)^2, j = \psi, z, \tag{8}$$

where p is the Laplace operator and $f_i(i = x, y, \psi, z)$ are positive constants. If $f_i(i = x, y, \psi, z)$ are sufficiently large, one can expect that these robust filters have sufficiently wide frequency bandwidths and thereby the gains of the filters would approximate to 1. The compensator control outputs are chosen as the lowpass-filtered disturbances as

$$u_i^R(p) = -F_i(p)\Delta_i(p), i = x, y, \psi, z. \tag{9}$$

From Eqs. 3 and 9, one can obtain the following state-space realization of the robust compensating input in the yaw subsystem

$$\dot{z}_{\psi 1} = -f_\psi z_{\psi 1} - \left(f_\psi^2 + a_{1\psi} f_\psi - a_{0\psi}\right) e_{\psi,1} + b_\psi u_\psi,$$

$$\dot{z}_{\psi 2} = -f_\psi z_{\psi 2} + (2 f_\psi - a_{1\psi})e_{\psi,1} + z_{\psi 1},$$

$$u_\psi^R = f_\psi^2(z_{\psi 2} - e_{\psi,1})/b_\psi. \tag{10}$$

From the above equations, one can see that the robust compensating input u_ψ^R does not depend on the uncertainties Δ_ψ. The realization of the robust compensating inputs in other subsystems can be achieved in similar ways. The whole schematic

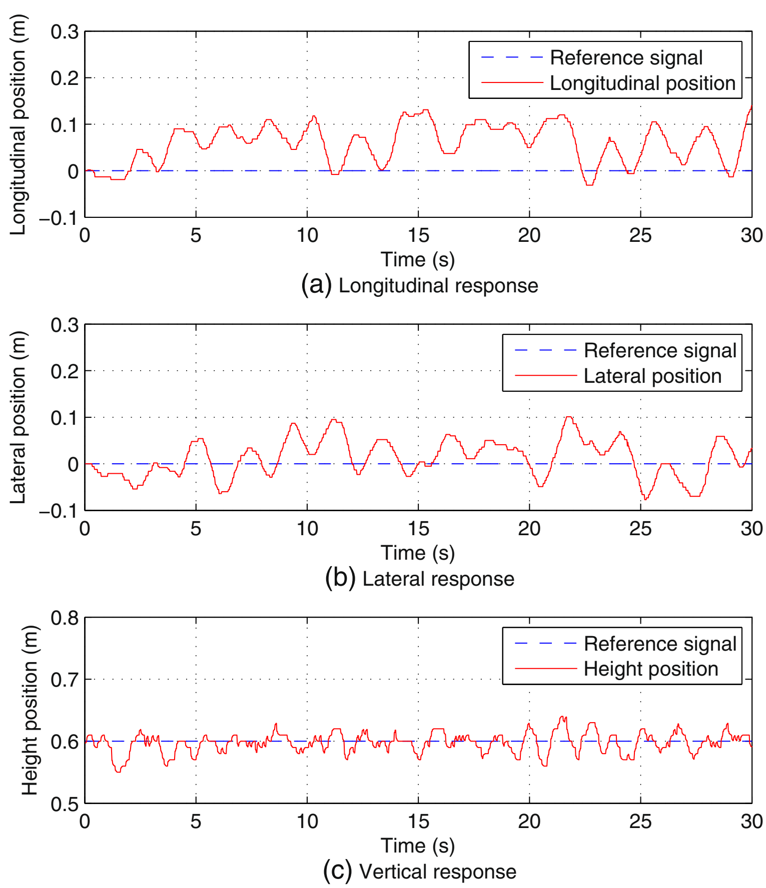

Fig. 4 Responses of the three positions in Case 1

diagram of the robust and decoupled control system is depicted in Fig. 3.

From Eqs. 6 and 10, one can see that, actually, a decoupled control is achieved for the four subsystems. For each subsystem, the nominal controller and robust compensator only depend on the own state feedback of the subsystem. Furthermore, the resulted controller is a linear time-invariant one, which is easily implementable in practical applications.

4 Robustness Property Analysis

In this section, the robust tracking properties of the whole closed-loop control system are analyzed. It will be shown that although a decoupled controller is designed, the tracking performance of the whole closed-loop system can still be guaranteed.

Theorem 1 *If the assumption presented in the second section can be met, then, for* a-priori *set constant* $\varepsilon > 0$ *and bounded initial state, there exist a constant* $T > 0$ *and parameters* $f_i > 0 (i = x, y, \psi, z)$ *with sufficiently large values, such that* e *is bounded and* $|e(t)| \leq \varepsilon, \forall t \geq T$.

Proof From Eqs. 5, 6, and 9, one can obtain that

$$\|u_i\|_\infty \leq \|K_i\|_1 \|e_i\|_\infty + \|\Delta_i\|_\infty, i = x, y, \psi, z. \quad (11)$$

Then, if Assumption 1 holds, it follows that

$$\|\Delta\|_\infty \leq \eta_{\Delta e} \|e\|_\infty + \eta_{\Delta c}, \quad (12)$$

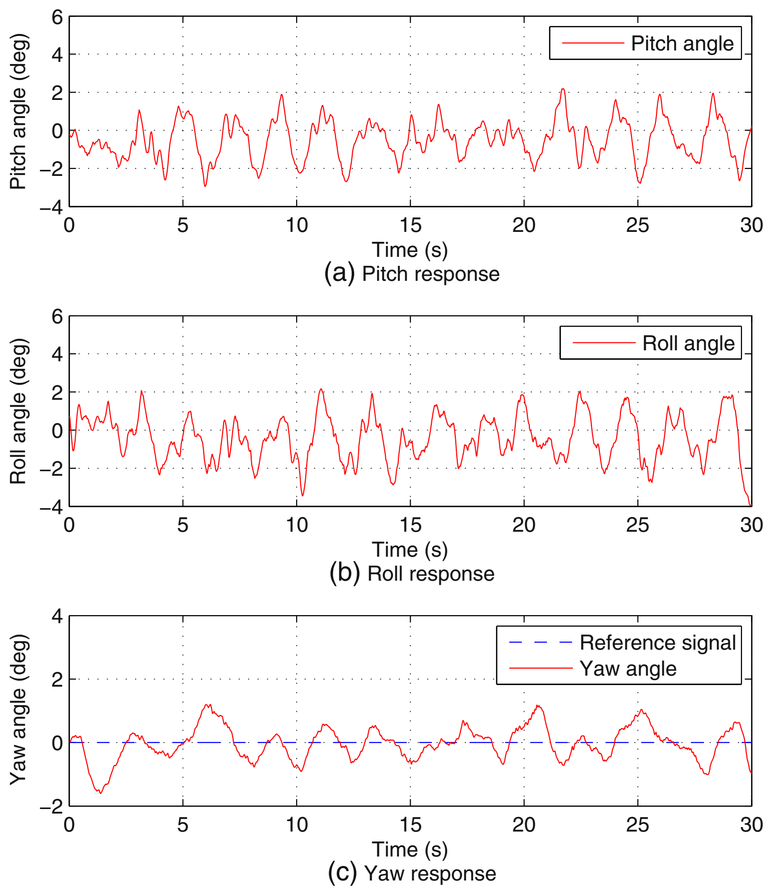

Fig. 5 Responses of the three Euler angles in Case 1

where

$$\eta_{\Delta e} = \max_i \frac{\varsigma_{ei} + \delta_i \|K_i\|_1}{1 - \delta_i}, \eta_{\Delta c} = \max_i \frac{\varsigma_{ci}}{1 - \delta_i}.$$

Moreover, from Eqs. 7 and 9, one can have that

$$\dot{e} = A_H e + B(I_{4\times 4} - F)\Delta, \tag{13}$$

where $A_H = diag(A_{xH}, A_{yH}, A_{\psi H}, A_{zH})$, $F = diag(F_x, F_y, F_\psi, F_z)$, and $I_{n\times n}$ is an $n \times n$ unit matrix. It follows that

$$\|e\|_\infty \le \eta_{e(0)} + \gamma \|\Delta\|_\infty, \tag{14}$$

where $\eta_{e(0)} = \max_k \sup_{t\ge 0} \left|c_k^T e^{A_H t} e(0)\right|$, c_k is a 12×1 vector with a one on the kth row and zeros elsewhere, and

$$\gamma = \left\|(sI_{12\times 12} - A_H)^{-1} B(I_{4\times 4} - F)\right\|_1.$$

If the robust compensator parameters $f_i (i = x, y, \psi, z)$ are sufficiently large, the gains of the robust filters F_i would approximate to 1. In this case, F would approximate to $I_{4\times 4}$ and thereby γ can be made as small as desired. Therefore, combining Eqs. 12 and 14, one has that

$$\|e\|_\infty \le (\eta_{e(0)} + \gamma \eta_{\Delta c})/(1 - \gamma \eta_{\Delta e}),$$

$$\|\Delta\|_\infty \le (\eta_{\Delta e} \eta_{e(0)} + \eta_{\Delta c})/(1 - \gamma \eta_{\Delta e}). \tag{15}$$

If $f_i (i = x, y, \psi, z)$ are sufficiently large and thus γ is made as small as desired, one can see that e is bounded (see, [16] and [17] to mention a few).

Now, from Eqs. 13 and 15, one can obtain that

$$\max_k |e_k(t)| \le \max_k \left|c_k^T e^{A_H t} e(0)\right| + \gamma \frac{\eta_{\Delta e} \eta_{e(0)} + \eta_{\Delta c}}{1 - \gamma \eta_{\Delta e}}.$$

Therefore, from the above expression, one can see that for *a-priori* set constant $\varepsilon > 0$ and the

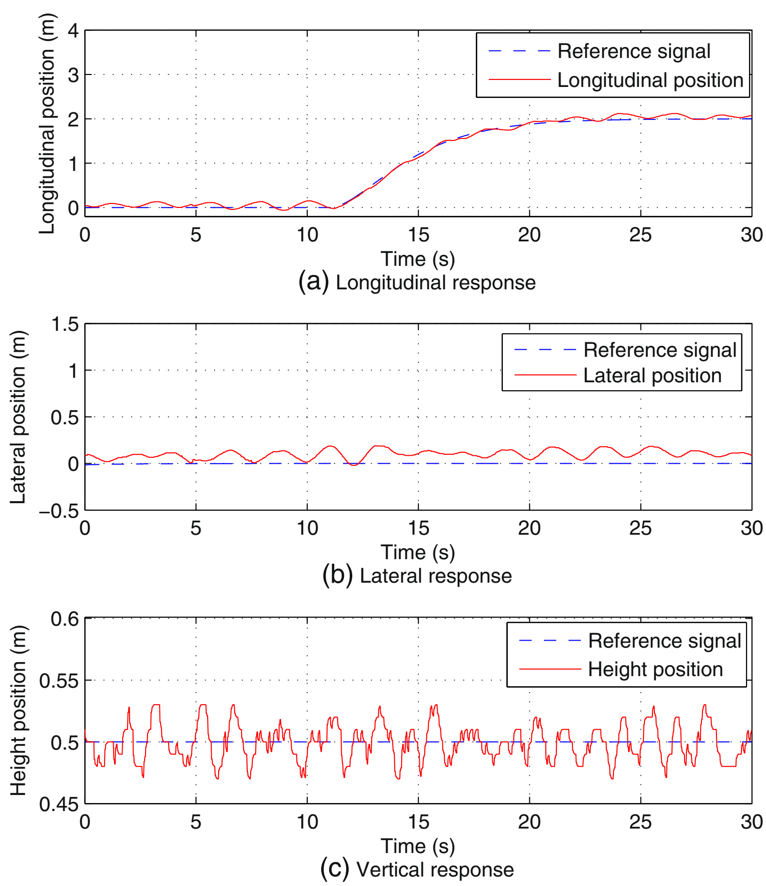

Fig. 6 Step responses for the longitudinal position in Case 2

bounded initial state, there exist a constant $T > 0$ and sufficiently large parameters $f_i > 0 (i = x, y, \psi, z)$, such that $|e(t)| \leq \varepsilon, \forall t \geq T$. □

5 Real-time Implementation of Decoupled Controller

Using the quadrotor systems as shown in Fig. 1, which is based on X-aircraft X650, real-time position control is experimented. An onboard avionic electronic system is added to obtain the attitude and position information and implement the proposed control algorithm. It includes three gyroscopes, a digital accelerometer, and a compass for the data fusion, and a TMS320 DSP for the automatic control. The nominal values of the helicopter parameters are shown as in Table 1. Moreover, the nominal controller parameters are chosen as: $K_x = \begin{bmatrix} 1 & 3 & 6 & 2 \end{bmatrix}$, $K_y = \begin{bmatrix} 1 & 3 & 6 & 2 \end{bmatrix}$, $K_\psi = \begin{bmatrix} 5 & 3 \end{bmatrix}$, and $K_z = \begin{bmatrix} 2.5 & 45 \end{bmatrix}$ by trial and error. The robust compensator parameters for each subsystem are selected as: $f_x = 1$, $f_y = 1$, $f_\psi = 1$, and $f_z = 1$ by tuning on-line.

5.1 Case1: Hovering Tests

The designed closed-loop control system is firstly tested for a hovering mission, where the reference values for the three positions and the yaw angle are $\{0\text{m}, 0\text{m}, 0.6\text{m}, 0\text{deg}\}$ respectively. Real-time experimental results of the three positions and three Euler angles are depicted in Figs. 4 and 5, respectively. From these figures, it can be seen that steady-state errors for the longitudinal, lateral, yaw, and height subsystems are maintained less than 0.15 m, 0.1 m, 2 deg, and 0.05 m respectively. The vehicle achieved promising hovering

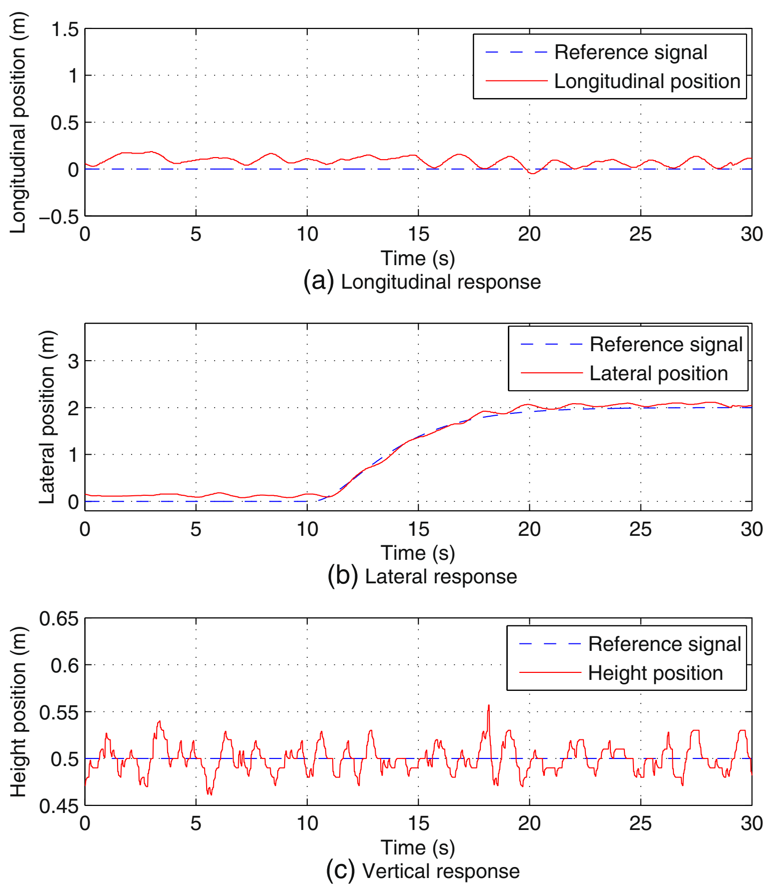

Fig. 7 Step responses for the lateral position in Case 2

performance considering the low-cost sensors and decoupled LTI models used.

5.2 Case 2: Step Responses

Then, the proposed closed-loop system is evaluated step responses. The longitudinal position is firstly needed to follow a step signal with the amplitude of 2 m, whereas the lateral and height positions are required to be stabilized at 0 m and 0.5 m respectively. Then, the lateral position is also required to track this signal and longitudinal and height positions are required to be stabilized at 0 m and 0.5 m respectively. Responses are shown in Figs. 6 and 7, respectively. From the figures, it can observed that desired step responses were tracked robustly and consistently by the proposed decoupled control method.

5.3 Case 3: Trajectory Tracking

In this case, the quadrotor is required to follow a horizontal circle with a radius of 1 m. The references of the height position and the yaw angle are set to be 1 m and 0 deg, respectively. Corresponding position responses and attitude angle responses are presented in Figs. 8 and 9 respectively. Good automatic flight results have been achieved.

6 Conclusions

A robust and decoupled controller was proposed for a six degrees of freedom quadrotor to achieve the automatic hovering and trajectory following. The quadrotor system was divided into four subsystems and a robust controller including a nominal controller and a robust compensator was

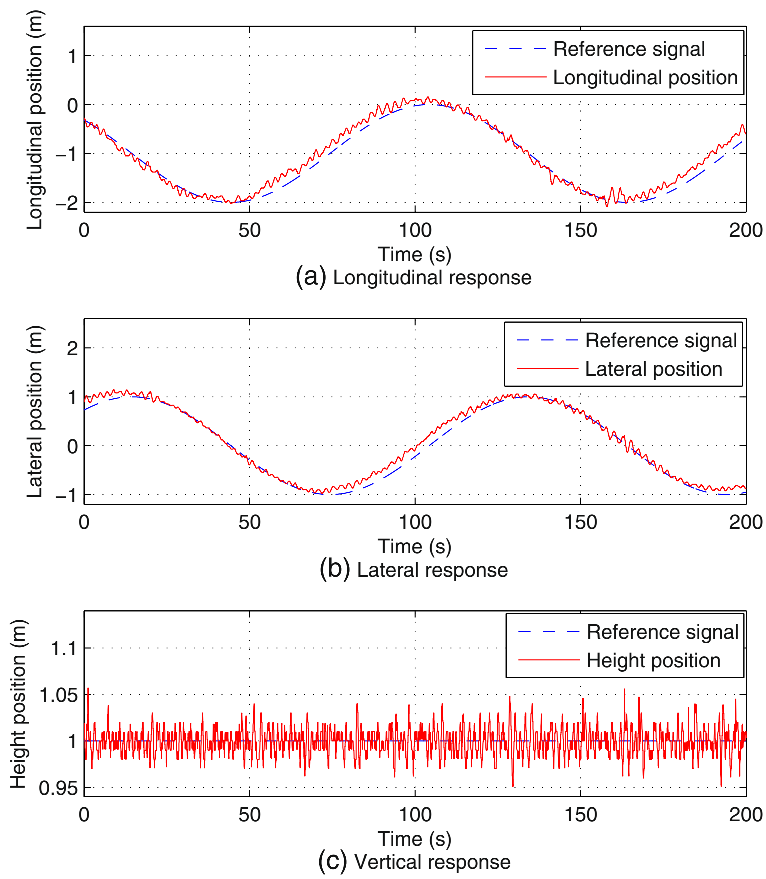

Fig. 8 Responses of the three positions in Case 3

Fig. 9 Responses of the three Euler angles in Case 3

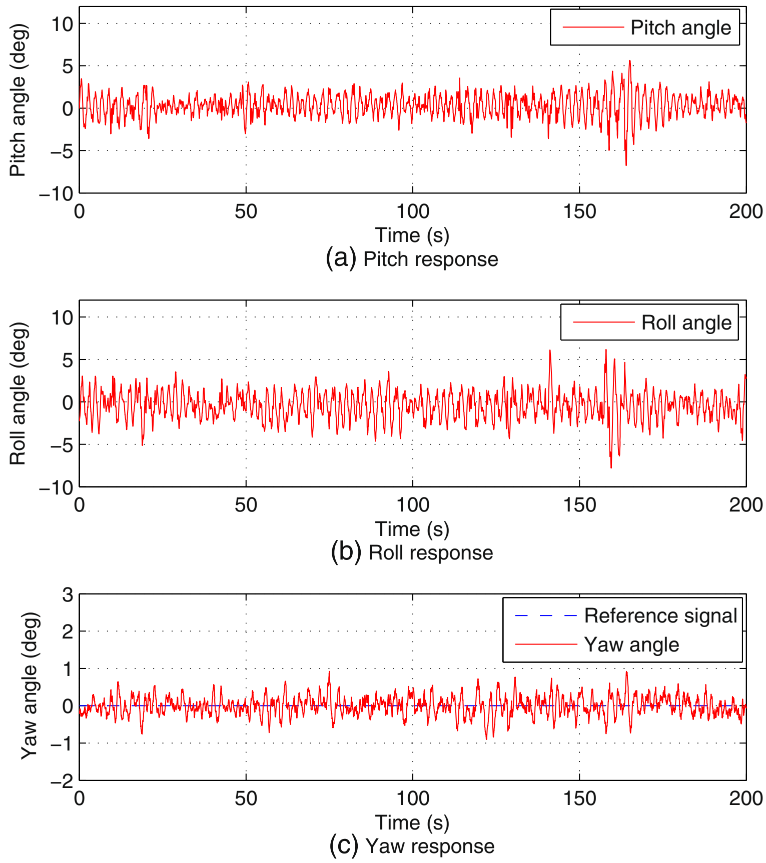

designed for each subsystem. Theoretical analysis was provided showing the convergence property of the closed-loop system and real-time experimental results demonstrate the viability and applicability of the proposed decoupled controller. Currently this method is being applied to more general multicopter models and tested under outdoor environments where wind disturbances are more severe.

Acknowledgements This work was supported by the National Natural Science Foundation of China under Grants 61174067, 61203071, and 61374054, as well as Shaanxi Province Natural Science Foundation Research Projection under Grants 2013JQ8038.

References

1. Gadewadikar, J., Lewis, F.L., Subbarao, K., Peng, K., Chen, B.M.: H-infinity static output-feedback control for rotorcraft. J. Intell. Robot. Syst. **54**(4), 629–646 (2009)
2. Liu, C., Chen, W., Andrews, J.: Tracking control of small-scale helicopters using explicit nonlinear MPC augmented with disturbance observers. Control Eng. Pract. **20**(3), 258–268 (2012)
3. Godbolt, B., Vitzilaios, N.I., Lynch, A.F.: Experimental validation of a helicopter autopilot design using model-based PID control. J. Intell. Robot. Syst. **70**(1–4), 385–399 (2013)
4. Raptis, I.A., Valavanis, K.P., Moreno, W.A.: A novel nonlinear backstepping controller design for helicopters using the rotation matrix. IEEE Trans. Control Syst. Technol. **19**(2), 465–473 (2011)
5. Das, A., Lewis, F., Subbarao, K.: Backstepping approach for controlling a quadrotor using Lagrange form dynamics. J. Intell. Robot. Syst. **56**(1–2), 127–151 (2009)
6. Hamel, T., Mahony, R.: Visual servoing of an under-actuated dynamic rigid-body system: an image-based approach. IEEE Trans. Robot. Autom. **18**(2), 187–198 (2002)
7. Castillo, P., Dzul, A., Lozano, R.: Real-time stabilization and tracking of a four-rotor mini rotorcraft. IEEE Trans. Control Syst. Technol. **12**(4), 510–516 (2004)
8. Altug, E., Ostrowski, J.P., Taylor, C.J.: Control of a quadrotor helicopter using dual camera visual feedback. Int. J. Robot. Res. **24**(5), 329–341 (2005)

9. Hoffmann, G.M., Huang, H., Waslander, S.L., Tomlin, C.J.: Quadrotor helicopter flight dynamics and control: theory and experiment. In: AIAA Guidance, Navigation and Control Conference and Exhibit, pp. 1–20. Hilton Head, South Carolina, USA (2007)
10. Pounds, P., Mahony, R., Corke, P.: Modelling and control of a large quadrotor robot. Control Eng. Pract. **18**(7), 691–699 (2010)
11. Bertrand, S., Guenard, N., Hamel, T., Piet-Lahanier, H., Eck, L.: A hierarchical controller for miniature VTOL UAVs: design and stability analysis using singular perturbation theory. Control Eng. Pract. **19**(10), 1099–1108 (2011)
12. Zuo, Z.: Trajectory tracking control design with command-filtered compensation for a quadrotor. IET Control Theory Appl. **4**(11), 2343–2355 (2010)
13. Zhang, R.: Attitude control of aquadrotor aircraft subject to a class of time-varying disturbances. IET Control Theory Appl. **5**(9), 1140–1146 (2011)
14. Guerrero-Castellanos, J.F., Marchand, N., Hably, A., Lesecq, S., Delamare, J.: Bounded attitude control of rigid bodies: real-time experimentation to a quadrotor mini-helicopter. Control Eng. Pract. **19**(8), 790–797 (2011)
15. Liu, H., Bai, Y., Lu, G., Shi, Z., Zhong, Y.: Robust tracking control of a quadrotor helicopter. J. Intell. Robot. Syst. (2013). doi:10.1007/s10846-013-9838-2
16. Zhong, Y.: Robust output tracking control of SISO plants with multiple operating points and with parametric and unstructured uncertainties. Int. J. Control. **75**(4), 219–241 (2002)
17. Liu, H., Lu, G., Zhong, Y.: Robust LQR attitude control of a 3-DOF lab helicopter for aggressive maneuvers. IEEE Trans. Ind. Electron. **60**(10), 4627–4636 (2013)